Mammalian and Fish Gelatin Methacryloyl–Alginate Interpenetrating Polymer Network Hydrogels for Tissue Engineering

Chen Ma, Ji-Bong Choi, Yong-Seok Jang, Seo-Young Kim, Tae-Sung Bae, Yu-Kyoung Kim,* Ju-Mi Park,* and Min-Ho Lee*

ACCESS | Metrics & More | Article Recommendations

ABSTRACT: Gelatin methacryloyl (GelMA) has been widely studied as a biomaterial for tissue engineering. Most studies focus on mammalian gelatin, but certain factors, such as mammalian diseases and diet restrictions, limit the use of mammalian gelatin. Thus, fish gelatin has received much attention as a substitute material in recent years. To develop a broadly applicable hydrogel with excellent properties, an interpenetrating polymer network (IPN) hydrogel was synthesized, since IPN hydrogels consist of at least two different hydrogel components to combine their advantages. In this study, we prepared GelMA using type A and fish gelatin and then synthesized IPN hydrogels using GelMA with alginate. GelMA single-network hydrogels were used as a control group. The favorable mechanical properties of type A and fish hydrogels improved after the synthesis of the IPN hydrogels. Type A and fish IPN hydrogels showed different mechanical properties (mechanical strength, swelling ratio, and degradation rate) and different cross-sectional morphologies, since the degree of mechanical enhancement in fish IPN hydrogels was less than that in type A; however, the cell biocompatibilities were not significantly different. Therefore, these findings could serve as a reference for future studies when selecting GelMA as a biological material for tissue engineering.
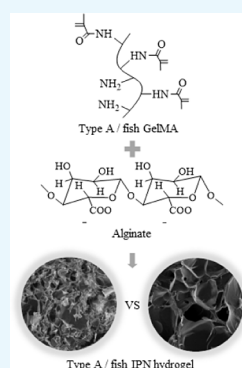
1. INTRODUCTION

Hydrogels have been widely used in tissue engineering recently, including in bone tissue scaffolds, contact lenses, wound healing dressings, and hygiene products because they show many characteristics similar to those of the extracellular matrix (ECM) of the body, including similar mechanical and biochemical properties.[1,2] Some physical properties of hydrogels, such as mechanical strength, swelling ratio, degradation rate, and pore size, have a significant influence on cell activities such as proliferation, elongation, differentiation, and migration.[3−6] Therefore, it is necessary to adjust the physical properties of the hydrogels according to the intended purpose, to meet the requirements of different applications of tissue engineering. The raw materials that make up the hydrogels have various physical, mechanical, and biological properties that can be obtained from natural or synthetic sources such as gelatin, sodium alginate (SA), polyacrylamide, chitosan, and hyaluronic acid (HA), among others.[7] For biomedical applications, naturally sourced polymers (gelatin, alginate, chitosan, etc.) are more suitable than synthetic polymers due to their excellent biocompatibility, low immune response, available bioactive motifs, and easy availability. Among these, gelatin is one of the most popular choices because of its similarity to ECM and many favorable properties such as biodegradability, good solubility, low antigenicity, low cost, low gelling point, and ease of manipulation; the most important property is that the abundant arginine−glycine−aspartic acid

(RGD) sequences in gelatin are good for cell adhesion, cell migration, and differentiation.[8] However, gelatin has some disadvantages such as rapid degradation and low mechanical modulus.[4,9,10] To overcome these drawbacks, some methods have been developed through chemical modification, such as methacrylation,[11] isocyanate incorporation,[12] and furfuryl-amine incorporation,[13] to enhance the mechanical properties. Methacrylation to modify gelatin (gelatin methacryloyl, GelMA) is the most common and effective of all these methods, and GelMA has been widely studied as a biomaterial; therefore, the main material selected for our study is GelMA. Numerous studies have confirmed that GelMA supports the adhesion and growth of various types of cells, such as mouse bone mesenchymal stem cells,[14,15] odontoblast-like cells,[16] neural stem cells,[17] human umbilical vein endothelial cells,[18] fibroblast cells,[19] and chondrocytes,[20] which benefit from the abundant RGD sequences as mentioned before. It has been well established that RGD sequences are most effective and widely employed for stimulated cell adhesion on synthetic surfaces, and RGD sequences inhibit cell adhesion to
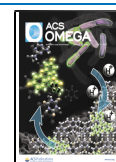
fibronectin while promoting cell adhesion on the synthetic surfaces through four steps, namely, cell attachment, cell spreading, organization of actin cytoskeleton, and formation of focal adhesions.[21] Many researchers focus on mammalian gelatin (type A gelatin and type B gelatin). For example, Koshy et al. fabricated injectable, porous, and cell-responsive gelatin cryogels using type A gelatin[22] and Vandervoort et al. constructed drug-loaded gelatin nanoparticles using type A and B gelatin for topical ophthalmic use.[23] But some factors like mammalian disease (e.g., bovine spongiform encephalopathy) and religious restrictions limit the use of mammalian gelatin and its further research.[22,24,25] Fish gelatin has received much attention as a substitute material in recent years, as it is free of mammalian diseases and faces less personal and religious limitations, compared with mammalian gelatin; however, some unfavorable mechanical properties, such as low mechanical modulus and rapid degradation, limit the application of fish gelatin as a biomaterial.[4,9]

An interpenetrating polymer network (IPN) hydrogels were designed to further develop the properties of the GelMA hydrogel. IPN hydrogels consist of at least two different hydrogel components to combine the advantageous characteristics of each polymer component.[6,25−27] Another type of hydrogel in the IPN hydrogel system used in this study is alginate, which is derived from brown algae and has favorable properties such as easy availability, biocompatibility, and gentle gelation. In this study, alginate was cross-linked with divalent ions (calcium ions), which is considered to be the most effective method. However, the application of alginate is often limited by some drawbacks, such as low elasticity, brittleness, low degradation rate, and poor bonding properties to cells because of the absence of ligands for mammalian cell attachment and low protein adsorption.[4,25,28−30] Therefore, previous studies modified alginate hydrogels by coupling RGD-containing peptides to the alginate backbone to enhance cell attachment.[31,32] Therefore, the IPN hydrogels developed in this study will be more biocompatible, with excellent mechanical properties, due to the combined advantages of both GelMA and alginate.

In this study, to develop a broadly applicable hydrogel with excellent properties for tissue engineering, IPN hydrogels were synthesized using type A or fish GelMA with SA. Finally, the compressive strength, cross-sectional morphology, swelling ratio, degradation rate, and biocompatibility of type A and fish IPN hydrogels were determined to compare their potentials as biomaterials for tissue engineering.

2. MATERIALS AND METHODS

2.1. Materials. Gelatin from porcine skin (Type A, 300 bloom, 50−100 kDa), gelatin from cold water fish skin (60 kDa), methacrylic anhydride (MA), and photoinitiator (2-hydroxy-4′-(2-hydroxyethoxy)-2-methylpropiophenone) were purchased from Sigma-Aldrich (MO, USA). SA (300−400 cP) was obtained from Wako (Osaka, Japanese).

2.2. Preparation of Samples. *2.2.1. Synthesis of GelMA.* Type A and fish GelMA were synthesized using the facile one-pot synthesis method according to the previous study (Figure 1a).[33] Briefly, 0.25 M CB buffer (100 mL) was made by dissolving sodium carbonate (7.95 g) and sodium bicarbonate (14.65 g) in distilled water, and then 10 g type A or fish gelatin was dissolved in 100 mL of 0.25 M CB buffer at 50°C, and 5 M sodium hydroxide was used to change the initial pH to 9. After that, 1 mL of MA was added to the gelatin solution and reacted
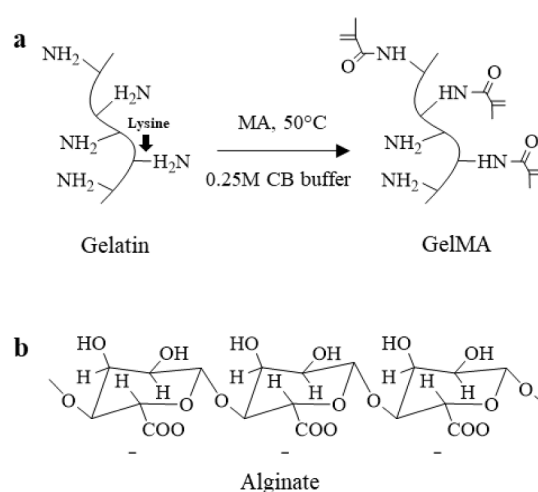

Figure 1. (a) Type A and fish gelatin were reacted with methacrylic anhydride (MA). (b) Molecular structure of alginate.

for 3 h under magnetic stirring at 50 °C. The reaction was stopped by changing the pH to 7.4 using 1 M hydrochloric acid. The potentially cytotoxic unreacted MA, salts, and byproducts in the reaction solution were removed through dialyzing against distilled water using the cutoff dialysis tube (12−14 kDa) at 40 °C for 7 days and changing fresh distilled water every day, filtered (0.22 μm filter), changed the pH to 7.4 using 1.5 M sodium hydroxide, and lyophilized. The final foamlike GelMA after freeze-drying was stored at −20 °C in the refrigerator until further use. GelMA from type A and fish gelatin was named A-GelMA and F-GelMA, respectively.

2.2.2. Evaluation of the Degree of Functionality. The degree of functionality (DoF) of GelMA was evaluated using ^{1}H NMR spectroscopy according to the previous studies.[34,35] ^{1}H NMR spectra were collected using a 600 MHz Fourier transform-NMR spectrometer (JNM-ECZ600R, JEOL, Japan) installed in the Center for University-Wide Research Facilities (CURF) at Jeonbuk National University. Fifty milligrams of gelatin and GelMA were dissolved in 1 mL deuterium oxide (D_2O) before the measurement, respectively. The DoF was investigated by calculating the percentage of ε-amino groups in gelatin that was modified in GelMA by reaction with MA using the following equation:[36]

$$DoF = 1 - \frac{\text{lysine methylene proton of GelMA}}{\text{lysine methylene proton of gelatin}} \times 100\%$$

2.2.3. Synthesis of GelMA Single-Network and SA/GelMA IPN Hydrogels. SA/GelMA IPN hydrogels were synthesized using three cross-link steps (Figure 2). Briefly, 2.5 w/v % SA and 20 w/v % GelMA were dissolved in PBS under 40 °C and mixed with 0.05 w/v % photoinitiator, respectively, and stored at 4°C overnight in the dark afterward. Following this treatment, the mixture was transferred to an incubator at 37 °C, which allowed GelMA and SA to fully dissolve without bubbles and turned clear. After that, 0.5 mL of SA solution, 0.5 mL of GelMA solution, and 22.3 μL of calcium sulfate slurry ($CaSO_4·2H_2O$, 0.21 g/mL) were mixed and injected onto a coverslip with 1 mm spacers immediately after mixing well. The mixture was allowed to gel for 30 min at room temperature on the coverslip. Finally, the mixed solution was turned into IPN hydrogels with the UV light source (WUV-L50, DAIHAN Scientific, South Korea) at 320−500 nm for 5
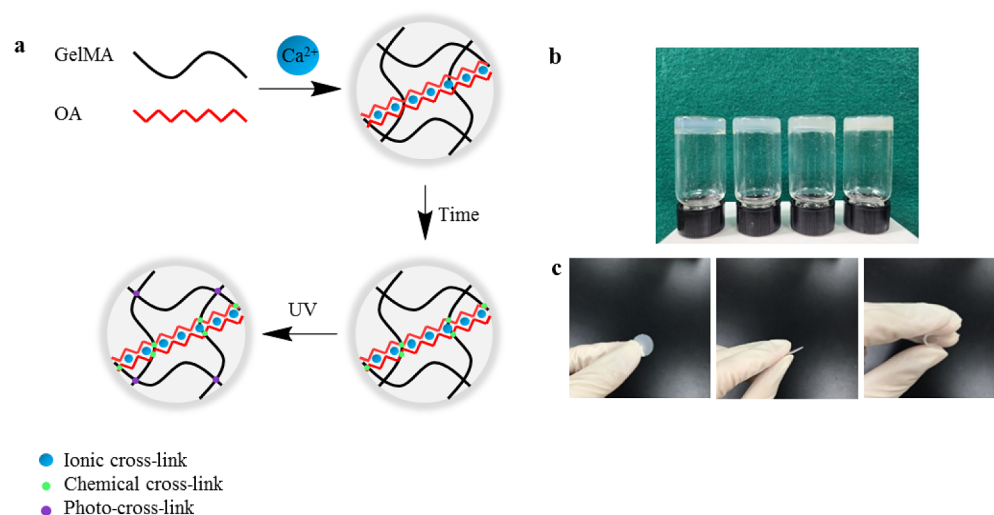
Figure 2. (a) Schematic of synthesizing SA/GelMA IPN hydrogels. (b) Digital photographs of hydrogels (from left to right: type A SN, fish SN, type A IPN, and fish IPN hydrogel). (c) Shape change of the hydrogel under stress.

min. The GelMA single network (SN) hydrogels were also synthesized using the same method as a control group.

2.3. Cross-Sectional Morphology. To identity the morphology of hydrogels, scanning electron microscopy (SEM) images were taken. Samples were immersed in PBS buffer at 37°C for 24 h to swell fully and then lyophilized overnight; after that, the cross-sections of dried hydrogels were prepared using a blade and coated with a thin layer of sputtered gold for 120 s. The cross-sectional morphology of the hydrogel samples was determined using a scanning electron microscope (JSM-5900, JEOL, Japan). ImageJ software (Nation Institutes of Health, Bethesda, MD, USA) was used to analyze the pore size and distribution through SEM images.[37,38]

2.4. Compressive Modulus Test. Before the compressive test, the hydrogel samples were immersed in PBS buffer to swell for 24 h; after that, a biopsy puncher was used to cut the sample into the shape of a cylinder (the diameter was 3 mm and the thickness was 1 mm). The mechanical testing of hydrogel disks was performed using a universal tester (GB 4201, Instron, UK) with 50 N load cell, the constant crosshead speed was 0.5 mm/min, and the sample number in each group was five. The compressive modulus was determined as the slope of the linear region corresponding to 5−15% strain in the stress−strain curve.

2.5. Swelling and Degradation Test. Sample disks were cut using a 10 mm diameter biopsy puncher after synthesizing hydrogels; there were five samples in each experimental group for the swelling and degradation test. First, the initial dry weights (W_i) of hydrogels (10 mm diameter and 1 mm thickness) were measured after freeze-drying overnight. Then, the freeze-dried hydrogel samples were immersed in PBS and incubated at 37 °C; PBS was replaced every week. The hydrogel samples were removed at several time points (1, 7, 14, and 21 days), were washed with fresh PBS, and absorbed the solution using Kim wipes on the sample surface. The weights of the samples in the swollen status (W_s) were recorded. The swelling ratio was calculated using the formula:

$$\text{swelling ratio} = W_s/W_i$$

After recording the hydrogel swollen weights, the samples were lyophilized again, and dry weight (W_d) after degradation

was measured. The mass loss ratio was calculated using the equation:[25]

$$\text{mass loss} = (W_i - W_d)/W_i \times 100\%$$

2.6. Cell Seeding and Characterization. The cell culture medium was prepared by adding 10% fetal bovine serum (FBS, Gibco Co., USA), 500 U/mL streptomycin (Gibco Co., USA), and 500 unit/mL penicillin (Gibco Co., USA) to α-minimal essential media (MEM, Gibco, Carlsbad, CA, USA). To avoid the cells to be dispersed in the well plate, the cylindrical hydrogels (15 mm × 1 mm) with a size matching the well plate (15 mm in diameter) were prepared as described before, sterilized using an autoclave, and inserted into the well plate; after that, the samples were cultured in the cell culture medium overnight in the incubator (37 °C and 5% CO_2). MC3T3-E1 (2×10^4 cells/mL) suspension was seeded on the hydrogel samples, and the culture medium was changed every 72 h. The cells cultured without the sample and with 0.1 M hydrogen peroxide acted as a negative and positive control group, respectively. After 3−5 days in culture, cell proliferation was determined using CCK-8 (Enzo Life Sciences Inc., NY, USA) assay for colorimetric analyses. Briefly, the cell culture medium was removed and fresh medium with 10% CCK-8 reagent was added; after that, the cells were further cultured at 37 °C in an incubator for 1.5 h. The formazan dye intensity was measured using an ELISA reader (Molecular Devices, EMax, San Jose, CA, USA) at a wavelength of 450 nm. Fluorescent staining of the cells was performed using the Live-Dead Cell Staining Kit (Enzo Life Sciences AG, Lausen, TX, USA) according to the manufacturer's instructions, and the live and dead image was determined using a superresolution confocal laser scanning microscope (LSM 880 with Airyscan, Carl Zeiss, Germany) installed in the Center for University-Wide Research Facilities (CURF) at the Jeonbuk National University.

2.7. Statistical Analysis. One-way analysis of variance (ANOVA) with a 95% confidence interval was performed to evaluate the statistical significance. The difference between two groups was considered statistically significant when the P-value was lower than 0.05. It was marked as *, **, *** when the P-value was less than 0.05, 0.01, and 0.001, respectively. All analyses were performed using GraphPad Prism 8.0.2 (Graph-
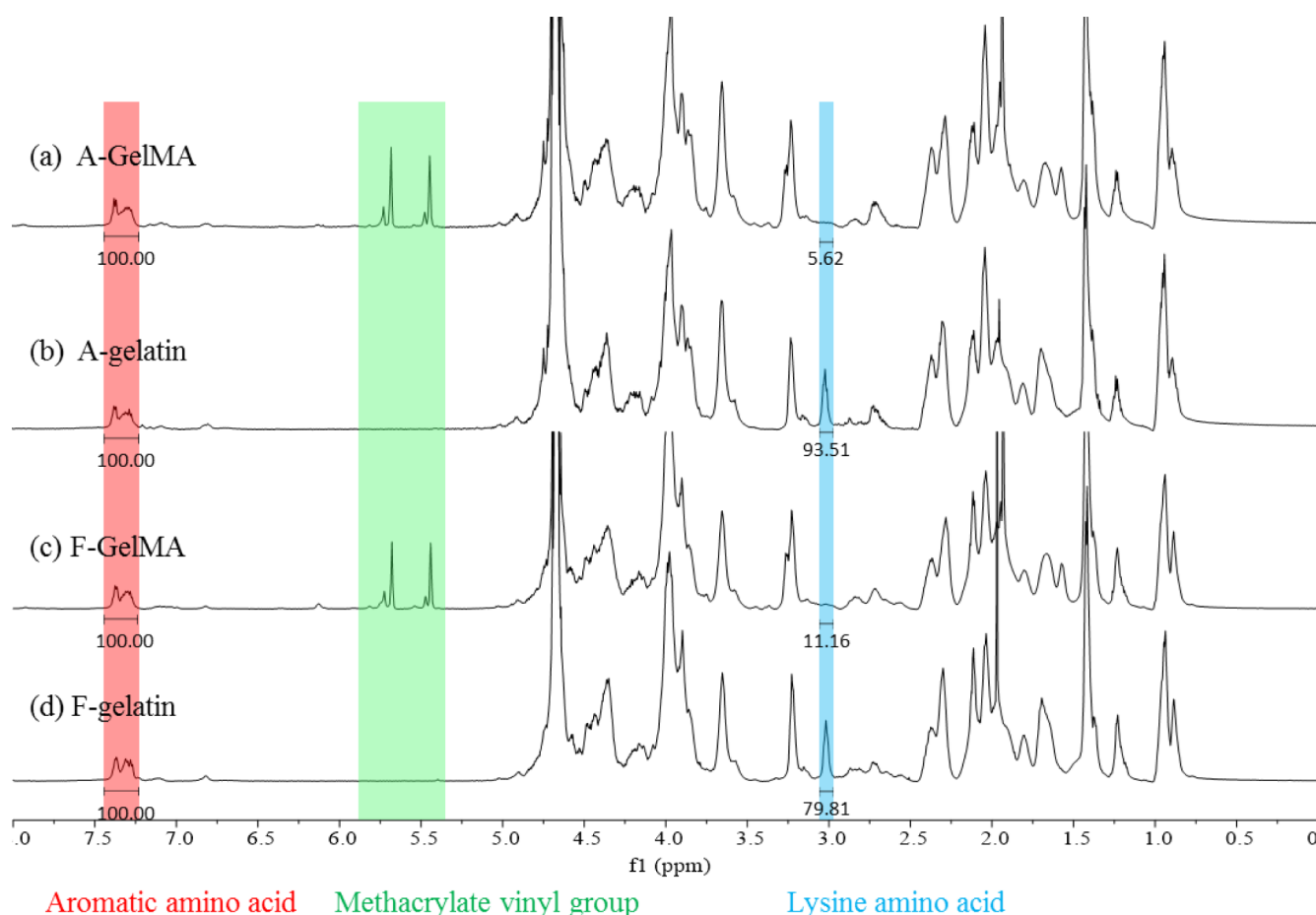
Figure 3. ^{1}H NMR spectra of type A and fish gelatin, GelMA macromers.

3. RESULTS

3.1. Synthesis of SN and IPN Hydrogels. The digital photographs of SN and IPN hydrogels are shown in Figure 2, and there was no significant difference between type A and fish hydrogels; however, the IPN hydrogels were opaquer than the SN hydrogels (Figure 2b). All types of hydrogel discs were transparent, flat, and elastic, and the shape of the hydrogels changed under force, but they returned to their original shape immediately when the force was removed (Figure 2c).

3.2. Degree of Functionality. The ^{1}H NMR spectra (Figure 3) were used to identify the methacrylamide groups in type A and fish GelMA. Compared with gelatin (Figure 3b,d), the new signals at δ = 5.4 and 5.7 ppm in GelMA (Figure 3a,c) were the protons of the methacrylate vinyl group of MA, the decreasing signal at δ = 2.9 ppm corresponded to the protons of methylene group of lysine, and the constant signal at δ = 7.3 ppm was an aromatic amino acid, so that the intensity of other protons in different samples was normalized by the intensity of the aromatic amino acid. The chemical structures of gelatin and GelMA are shown in Figure 1a. The new functional groups that were modified from lysine were formed in the GelMA attributed to the reaction between gelatin and MA; it caused the decrease in the intensity of lysine. Therefore, the DoF was calculated by comparing the proton integral value (δ = 2.9 ppm) of GelMA lysine residues with the lysine proton integral of untreated gelatin, using MestReNova 12.0.2 (Mestrelab

Research S. L., Santiago de Compostela, Spain). The DoFs of A-GelMA and F-GelMA were 94% and 86%, respectively (Table 1).

Table 1. DoF of Type A and Fish GelMA

group	DoF (%)
A-GelMA	94
F-GelMA	86

3.3. Cross-Sectional Morphology. The cross-sectional morphology of the hydrogels was observed using SEM (Figure 4A). The samples were dried by lyophilization before SEM analysis. Although the structure of the freeze-dried hydrogels is different from that of the wet state before lyophilization, it is still an intuitive and effective method for observing the morphology of the hydrogel cross-section. All hydrogel samples showed the porous cross-sectional morphology, and the detailed information of pore size and distribution is presented in Figure 4B. The mean pore diameters of type A and fish SN hydrogels were 141.1 ± 72.6 μm and 198.1 ± 125.9 μm (Figure 4B-a,B-b), respectively. However, the mean diameter of the pores was significantly decreased after blending with alginate to form IPN hydrogels with either type A or fish hydrogels. The mean diameter of type A and fish IPN hydrogels was 23.3 ± 18.4 and 88.2 ± 46 μm (Figure 4B-c,B-d), respectively. Furthermore, the pores of type A hydrogels were smaller and denser than those of fish IPN hydrogels, as evident in the SEM images.
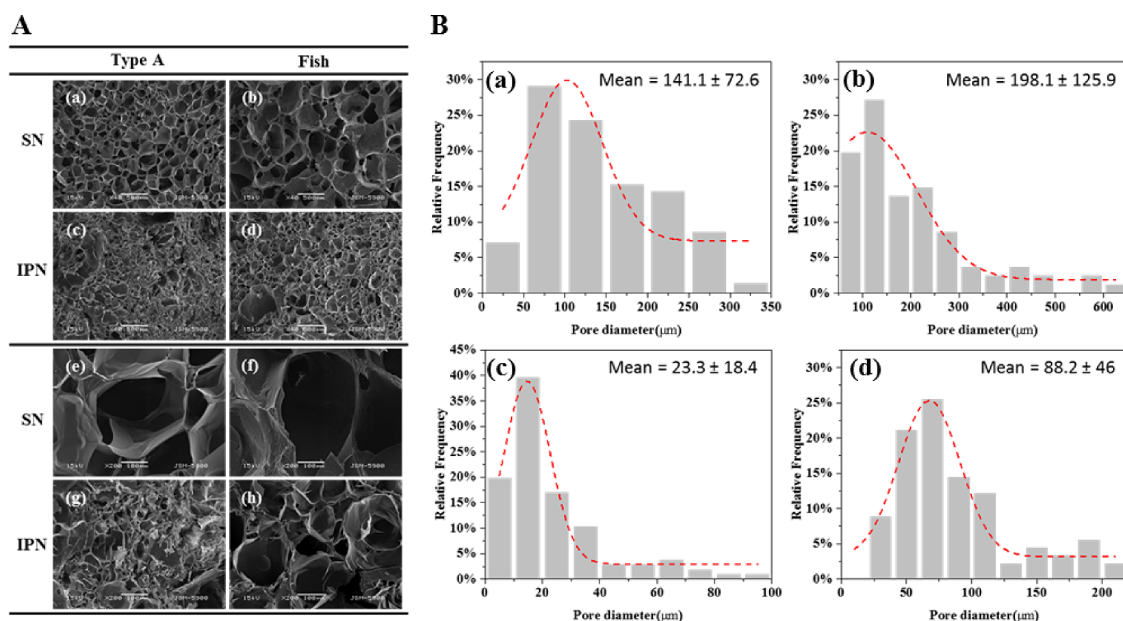
Figure 4. (A) Images of the cross-sectional morphology of type A SN (a, e), fish SN (b, f), type A IPN (c, e), and fish IPN (d, h) hydrogels were obtained using scanning electron microscopy. Images (e), (f), (g), and (h) are the images (a), (b), (c), and (d) at high magnification, respectively. (B) Analysis of pore size and distribution of type A SN (a), fish SN (b), type A IPN (c), and fish IPN (d) hydrogels (the unit of the mean diameter of the pores is in micrometer).
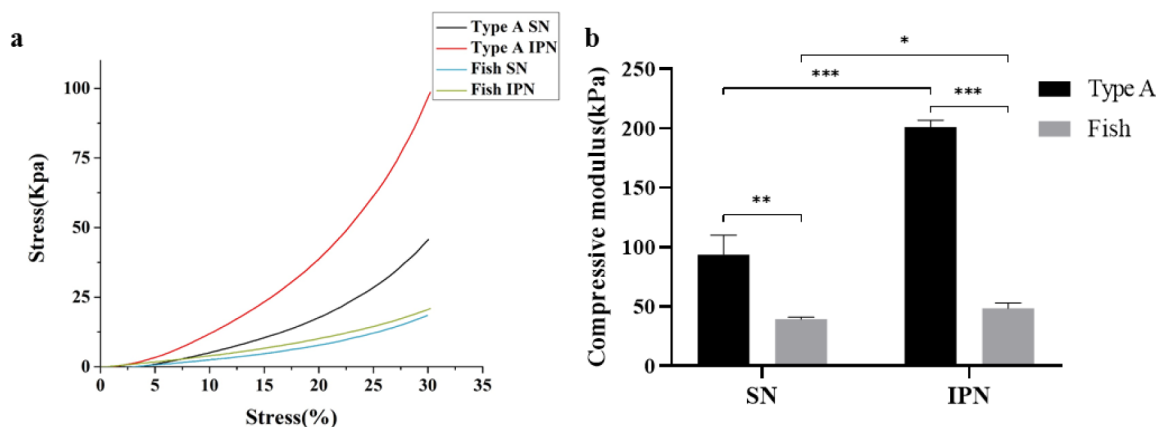

Figure 5. Stress−strain curve of the compression test (a) and analysis of the compressive modulus (b) of type A SN, fish SN, type A IPN, and fish IPN hydrogels. Error bars represent SDs of measurements performed on five samples ($*P < 0.05$, $**P < 0.01$, $***P < 0.001$).
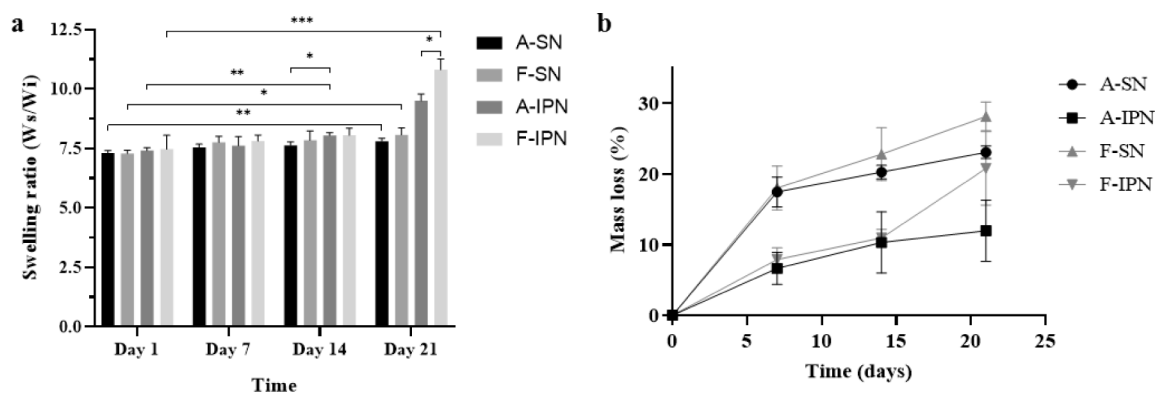
Figure 6. Swelling ratio (a) and degradation rate (b) of type A SN, fish SN, type A IPN, and fish IPN hydrogels. The swelling ratio and mass loss change were determined after immersing different hydrogels in PBS for 21 days.

3.4. Mechanical Modulus. To determine the difference between type A and fish IPN hydrogels on the mechanical modulus, an unconfined compressive test was performed. The compressive modulus (Figure 5b) was calculated using the
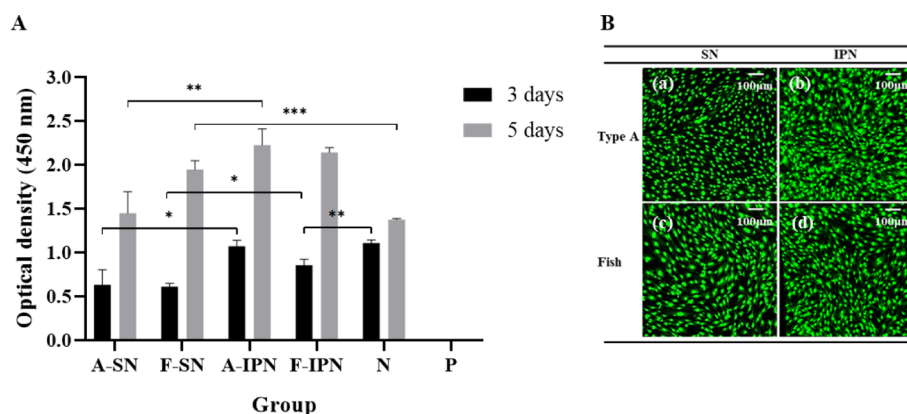
Figure 7. (A) The proliferation of MC3T3-E1 cells seeded on type A SN, fish SN, type A IPN, and fish IPN hydrogels for 3 and 5 days (N, negative control group; P, positive control group; $*P < 0.05$, $**P < 0.01$, $***P < 0.001$). (B) Fluorescence microscopy images of adhesion of MC3T3-E1 cells on type A (a, b) and fish (c, d) SN and IPN hydrogels after 5 days.

stress–strain curve (Figure 5a). The compressive modulus of type A hydrogels was significantly higher than that of fish hydrogels in SN or IPN hydrogels, but they showed a similar trend of change after the formation of IPN hydrogels. Compared with SN hydrogels, the compressive modulus was significantly increased from 93.6 ± 16.6 to 201.2 ± 5.5 kPa in type A hydrogel and slightly increased from 39.4 ± 1.7 to 48.6 ± 4.7 kPa in fish hydrogel after the synthesis of IPN hydrogels using GelMA and alginate.

3.5. Swelling and Degradation. The stability (swelling and degradation) of hydrogels is an important factor to be considered for tissue engineering and medical applications; therefore, it is essential to investigate the stability of hydrogels. As shown in Figure 6a, there was no significant difference in the swelling ratios of type A SN and IPN hydrogels until 7 days, but type A IPN hydrogels showed a higher swelling ratio than SN hydrogels after 14 days, and the difference was even more significant after 21 days. Fish hydrogels showed similar results, but the difference in swelling ratios of fish SN and IPN hydrogels was observed after 21 days. Furthermore, there was no significant difference between the swelling ratio of type A SN hydrogels and fish SN hydrogels for 21 days, but after the synthesis of IPN hydrogels, fish IPN hydrogels had a significantly higher swelling ratio than type A hydrogels after 21 days. The mass loss in Figure 6b represents the degradation rate; the degradation rate of type A and fish hydrogels decreased after the synthesis of IPN hydrogels, and it was relatively higher in fish hydrogels compared with that in type A hydrogels. After being immersed in PBS for 21 days, the mass loss was $23\% \pm 0.8\%$ (type A SN), $12\% \pm 3.9\%$ (type A IPN), $28.1\% \pm 1.8\%$ (fish SN), and $20.8\% \pm 4.7\%$ (fish IPN).

3.6. Cell Viability. To determine the effect of different hydrogels on cell viability, cell proliferation was assessed using the WST assay (Figure 7A). Cell proliferation improved after synthesis of IPN hydrogels, but there was no significant difference in cell proliferation in the case of type A and fish IPN hydrogels during culturing for 5 days. Furthermore, except for type A IPN hydrogels, all other hydrogels showed lower cell viability compared with the negative control group after 3 days; however, all groups presented similar or even higher cell viability than the negative control group after culturing for 5 days. To observe the number of cells attached to the hydrogels more clearly, fluorescent staining was performed according to the manufacturer's instructions after 5 days. All hydrogels showed many cells adhered on the surface, and the cells were mainly stained green (Figure 7B).

4. DISCUSSION

The SA/GelMA IPN hydrogels were prepared through three cross-linking steps, as shown in Figure 2. Alginate contains blocks of (1,4)-linked β-D-mannuronate (M) and α-L-guluronate (G) residues; however, only the G-blocks can be cross-linked with divalent cations to form hydrogels,[30] and the G-blocks of alginate in the IPN hydrogel system were cross-linked by Ca^{2+} ions to form a single cross-link. Subsequently, alginate and GelMA were intertwined together through the formation of the imine bond, through the Schiff base reaction between the aldehyde groups of the SA and the amine group of GelMA, leading to dual cross-linking.[39−41] Finally, GelMA was formed by covalently cross-linked hydrogels under UV light exposure in the presence of the photoinitiator, resulting in triple-cross-linking. The presence of a stiff triple-cross-linked network is the main reason why the SA/GelMA IPN hydrogels showed far better physical properties than GelMA SN hydrogels. Generally, the compressive modulus of GelMA hydrogels depends on the molecular weight and cross-linking density by the available cross-link groups. It has been reported by Young that type A unmodified gelatin had more available free amines than fish gelatin;[42] therefore, the higher compressive modulus was observed in the IPN hydrogel, which has more cross-linking density synthesized by type A gelatin. Furthermore, the influence of the DoF of GelMA on the mechanical properties has been studied by many researchers. Generally, GelMA with a high DoF shows some excellent mechanical properties. For example, Nichol fabricated a hydrogel for microscale tissue engineering using GelMA,[11] and the results showed that the physical properties of fabricated GelMA hydrogels can be controlled by varying the DoF, and the compressive modulus of GelMA hydrogels was significantly higher with high (81.4 ± 0.4) DoF compared to that with medium (53.8 ± 0.5) and low (19.7 ± 0.7) DoF. To fabricate a strong hydrogel, type A and fish GelMA were synthesized by a facile one-pot method to achieve a high DoF in this study. The amount of methacrylamide groups, methacrylate, and its byproduct (methacrylic acid) in GelMA was determined by ^{1}H NMR (Figure 3) to identify the DoF. The DoF of A-GelMA (94%) was higher than that of F-GelMA

(86%) in this study, which is one of the reasons why type A hydrogels are far stiffer than fish hydrogels.

The cross-sectional morphology of the hydrogels was analyzed by SEM. The porous structure can be clearly observed in the SEM images, and it has a significant effect on the compressive properties of hydrogels.[43,44] Generally, a thinner network wall and lower polymer volume density is found in hydrogels with large pore size, leading to low mechanical strength.[45] As shown in Figure 4, the pore size of type A and fish IPN hydrogels was significantly decreased in comparison with that in SN hydrogels, due to the addition of alginate, and greatly increased cross-linking density because of triple cross-linking. Hence, the IPN hydrogels were much stronger than SN hydrogels. Figure 4Ag,h shows that the pores of type A IPN hydrogels were smaller and denser than those of the fish IPN hydrogels. The reason is also relative to the higher cross-linking density and higher DoF of type A GelMA,[46] which is the same as that of compressive modulus; therefore, type A IPN hydrogels had a relatively higher modulus of strength than fish IPN hydrogels (Figure 5b). The swelling ratio test was performed to investigate the water retention of hydrogels, and the swelling properties of hydrogels depend on the hydrogel density of cross-linking, polymer chain stiffness, polymer concentration, interaction with solvents, etc. As shown in Figure 6a, the type A and fish IPN hydrogels had a greater swelling ratio than SN hydrogels after immersion in PBS for several weeks, due to the presence of the carboxylate groups in alginate with a great hydrophilic character.[47] A significant difference between the swelling ratios of SN and IPN hydrogels appeared in type A hydrogels after 14 days and in fish hydrogels after 21 days. Type A and fish SN hydrogels had similar swelling ratios after immersion in PBS for 21 days, but after the addition of alginate, fish IPN hydrogels had a higher swelling ratio than type A IPN hydrogels after 21 days, because the pore size of the fish IPN hydrogels was larger than that of the type A IPN hydrogels (Figure 4B-c,B-d).

Hydrogel has been studied as a biomaterial with applications in tissue engineering, and its degradation rate needs to be optimized according to the target tissue. Fast degradation, a drawback of the GelMA single network hydrogel was overcome by combining the advantageous characteristics of GelMA and alginate to synthesize IPN hydrogels. As shown in Figure 6b, the lifetime of type A and fish IPN hydrogels was longer than that of the SN hydrogels because alginate led to a high cross-linking density in the IPN hydrogel system. Furthermore, fish IPN hydrogels had a relatively higher degradation rate than type A IPN hydrogels because of their large and loose porous structure.

Hydrogels have been used as biomaterials in various applications, such as wound dressing, artificial vessels, and tissue implants, which are directly in contact with tissue or inserted into the body.[48−50] Therefore, the cell compatibility of hydrogels is crucial in tissue engineering.[51,52] The effect of different hydrogel materials on cell biocompatibility was investigated in this study. According to the WST assay (Figure 7A), synthesizing type A and fish IPN hydrogels accelerated cell proliferation due to the high swelling ratio of IPN hydrogels, which greatly enables the transport of nutrients, oxygen, and metabolites to the cell.[53] An interesting phenomenon can be found that cell viability was similar between SN and IPN hydrogel after 5 days in the fish group; the most plausible reason could be that the population of cells in the fish SN group already reached a very high value after 5

days, so that there was a slight increase in cell proliferation in the fish IPN hydrogel group compared with that in the fish SN hydrogel group affected by contact inhibition between adjacent cells caused by the high cell density.[54] There was no significant difference in cell proliferation between type A and fish IPN hydrogels during culturing for 5 days. In addition, there was no negative effect of hydrogels on cell viability after 5 days, which indicated that the proliferation of cells was not inhibited by the presence of hydrogels, although it showed a lower cell viability than the negative control group on the third day of cell culture; this phenomenon has also been observed in other studies.[55] Furthermore, the high cell viability in all groups was also evident in the fluorescence microscopy images (Figure 7B), which indicated that the materials and processes of type A and fish IPN hydrogel synthesis were free of obvious toxicity.

Although, the use of fish-derived GelMA has been studied previously,[9,42,56] it is difficult to compare the properties of type A and fish GelMA−alginate IPN hydrogels because the cross-link conditions are quite different between each previous study. This study compared the physical and biological performance of type A and fish IPN hydrogels under the same conditions, and the findings could serve as a reference for future studies when selecting GelMA as a biological material for tissue engineering.

5. CONCLUSIONS

In this study, we synthesized type A and fish IPN hydrogels using alginate and GelMA, with GelMA single network hydrogels as control. Type A and fish hydrogels were compared in terms of the DoF, cross-sectional morphology, compressive modulus, swelling ratio, degradation, and cell compatibility, assuming fish type as one of the candidate materials that can be used as an alternative to type A hydrogels.

The mechanical properties of type A and fish hydrogels improved after the synthesis of IPN hydrogels by GelMA and alginate. Fish IPN hydrogels showed a lower compressive modulus, higher swelling ratio, and faster degradation than type A IPN hydrogels, because of the larger pore size; however, there was no difference between the two groups for 14 days in swelling and degradation evaluation. In addition, there was a positive effect of type A and fish hydrogels on cell viability after 5 days, indicating that the process of type A and fish IPN hydrogel synthesis was free of obvious toxicity. Overall, the fish IPN hydrogel also showed significant improvements in terms of mechanical and physical properties and biocompatibility compared to SN hydrogels.

■ AUTHOR INFORMATION

Corresponding Authors

Yu-Kyoung Kim − *Department of Dental Biomaterials, Institute of Biodegradable Materials, School of Dentistry, Jeonbuk National University, Jeonju-si 54896, Jeollabuk-do, South Korea*; Email: yk0830@naver.com

Ju-Mi Park − *Department of Prosthodontics, School of Dentistry, Jeonbuk National University, Jeonju 54896, South Korea*; Email: jmpark@jbnu.ac.kr

Min-Ho Lee − *Department of Dental Biomaterials, Institute of Biodegradable Materials, School of Dentistry, Jeonbuk National University, Jeonju-si 54896, Jeollabuk-do, South Korea*; ⓘ orcid.org/0000-0001-6142-4876; Email: mh@jbnu.ac.kr

Authors

Chen Ma − *Department of Dental Biomaterials, Institute of Biodegradable Materials, School of Dentistry, Jeonbuk National University, Jeonju-si 54896, Jeollabuk-do, South Korea*

Ji-Bong Choi − *Department of Dental Biomaterials, Institute of Biodegradable Materials, School of Dentistry, Jeonbuk National University, Jeonju-si 54896, Jeollabuk-do, South Korea*

Yong-Seok Jang − *Department of Dental Biomaterials, Institute of Biodegradable Materials, School of Dentistry, Jeonbuk National University, Jeonju-si 54896, Jeollabuk-do, South Korea*

Seo-Young Kim − *Department of Dental Biomaterials, Institute of Biodegradable Materials, School of Dentistry, Jeonbuk National University, Jeonju-si 54896, Jeollabuk-do, South Korea*

Tae-Sung Bae − *Department of Dental Biomaterials, Institute of Biodegradable Materials, School of Dentistry, Jeonbuk National University, Jeonju-si 54896, Jeollabuk-do, South Korea;* ⓘ orcid.org/0000-0002-8307-4544

Complete contact information is available at:
https://pubs.acs.org/10.1021/acsomega.1c01806

Notes

The authors declare no competing financial interest.

■ REFERENCES

(1) Choi, Y. H.; Kim, S. H.; Kim, I. S.; Kim, K.; Kwon, S. K.; Hwang, N. S. Gelatin-based micro-hydrogel carrying genetically engineered human endothelial cells for neovascularization. *Acta Biomater.* **2019**, *95*, 285−296.

(2) Shin, H.; Olsen, B. D.; Khademhosseini, A. The mechanical properties and cytotoxicity of cell-laden double-network hydrogels based on photocrosslinkable gelatin and gellan gum biomacromolecules. *Biomaterials* **2012**, *33*, 3143−3152.

(3) Wang, Y. H.; Ma, M.; Wang, J. N.; Zhang, W. J.; Lu, W. P.; Gao, Y. H.; Zhang, B.; Guo, Y. C. Development of a photo-crosslinking, biodegradable GelMA/PEGDA hydrogel for guided bone regeneration materials. *Materials* **2018**, *11*, No. 1345.

(4) Zhang, X.; Kim, G. J.; Kang, M. G.; Lee, J. K.; Seo, J. W.; Do, J. T.; Hong, K.; Cha, J. M.; Shin, S. R.; Bae, H. Marine biomaterial-based bioinks for generating 3D printed tissue constructs. *Mar. Drugs* **2018**, *16*, No. 484.

(5) Chen, C. H.; Kuo, C. Y.; Wang, Y. J.; Chen, J. P. Dual function of glucosamine in gelatin/hyaluronic acid cryogel to modulate scaffold mechanical properties and to maintain chondrogenic phenotype for cartilage tissue engineering. *Int. J. Mol. Sci.* **2016**, *17*, No. 1957.

(6) Suo, H. R.; Zhang, D. M.; Yin, J.; Qian, J.; Wu, Z. L.; Fu, J. Z. Interpenetrating polymer network hydrogels composed of chitosan and photocrosslinkable gelatin with enhanced mechanical properties for tissue engineering. *Mater. Sci. Eng., C* **2018**, *92*, 612−620.

(7) Caliari, S. R.; Burdick, J. A. A practical guide to hydrogels for cell culture. *Nat. Methods* **2016**, *13*, 405−414.

(8) Mao, D. Y.; Li, Q.; Li, D. K.; Tan, Y.; Che, Q. J. 3D porous poly(epsilon-caprolactone)/58S bioactive glass-sodium alginate/gelatin hybrid scaffolds prepared by a modified melt molding method for bone tissue engineering. *Mater. Des.* **2018**, *160*, 1−8.

(9) Yoon, H. J.; Shin, S. R.; Cha, J. M.; Lee, S. H.; Kim, J. H.; Do, J. T.; Song, H.; Bae, H. Cold water fish gelatin methacryloyl hydrogel for tissue engineering application. *PLoS One* **2016**, *11*, No. e0163902.

(10) Kwon, S.; Lee, S. S.; Sivashanmugam, A.; Kwon, J.; Kim, S. H. L.; Noh, M. Y.; Kwon, S. K.; Jayakumar, R.; Hwang, N. S. Bioglass-incorporated methacrylated gelatin cryogel for regeneration of bone defects. *Polymers* **2018**, *10*, No. 914.

(11) Nichol, J. W.; Koshy, S. T.; Bae, H.; Hwang, C. M.; Yamanlar, S.; Khademhosseini, A. Cell-laden microengineered gelatin methacrylate hydrogels. *Biomaterials* **2010**, *31*, 5536−5544.

(12) Tronci, G.; Neffe, A. T.; Pierce, B. F.; Lendlein, A. An entropy-elastic gelatin-based hydrogel system. *J. Mater. Chem.* **2010**, *20*, 8875−8884.

(13) Son, T. I.; Sakuragi, M.; Takahashi, S.; Obuse, S.; Kang, J.; Fujishiro, M.; Matsushita, H.; Gong, J. S.; Shimizu, S.; Tajima, Y.; Yoshida, Y.; Suzuki, K.; Yamamoto, T.; Nakamura, M.; Ito, Y. Visible light-induced crosslinkable gelatin. *Acta Biomater.* **2010**, *6*, 4005−4010.

(14) Zheng, J. F.; Zhao, F. J.; Zhang, W.; Mo, Y. F.; Zeng, L.; Li, X.; Chen, X. F. Sequentially-crosslinked biomimetic bioactive glass/gelatin methacryloyl composites hydrogels for bone regeneration. *Mater. Sci. Eng., C* **2018**, *89*, 119−127.

(15) Celikkin, N.; Mastrogiacomo, S.; Jaroszewicz, J.; Walboomers, X. F.; Swieszkowski, W. Gelatin methacrylate scaffold for bone tissue engineering: the influence of polymer concentration. *J. Biomed. Mater. Res., Part A* **2018**, *106*, 201−209.

(16) Monteiro, N.; Thrivikraman, G.; Athirasala, A.; Tahayeri, A.; Franca, C. M.; Ferracane, J. L.; Bertassoni, L. E. Photopolymerization of cell-laden gelatin methacryloyl hydrogels using a dental curing light for regenerative dentistry. *Dent. Mater.* **2018**, *34*, 389−399.

(17) Lee, Y.; Lee, J. M.; Bae, P. K.; Chung, I. Y.; Chung, B. H.; Chung, B. G. Photo-crosslinkable hydrogel-based 3D microfluidic culture device. *Electrophoresis* **2015**, *36*, 994−1001.

(18) Nikkhah, M.; Eshak, N.; Zorlutuna, P.; Annabi, N.; Castello, M.; Kim, K.; Dolatshahi-Pirouz, A.; Edalat, F.; Bae, H.; Yang, Y. Z.; Khademhosseini, A. Directed endothelial cell morphogenesis in micropatterned gelatin methacrylate hydrogels. *Biomaterials* **2012**, *33*, 9009−9018.

(19) Wang, Z. J.; Kumar, H.; Tian, Z. L.; Jin, X.; Holzman, J. F.; Menard, F.; Kim, K. Visible light photoinitiation of cell-adhesive gelatin methacryloyl hydrogels for stereolithography 3D bioprinting. *ACS Appl. Mater. Interfaces* **2018**, *10*, 26859−26869.

(20) Bartnikowski, M.; Bartnikowski, N. J.; Woodruff, M. A.; Schrobback, K.; Klein, T. J. Protective effects of reactive functional groups on chondrocytes in photocrosslinkable hydrogel systems. *Acta Biomater.* **2015**, *27*, 66−76.

(21) Hersel, U.; Dahmen, C.; Kessler, H. RGD modified polymers: biomaterials for stimulated cell adhesion and beyond. *Biomaterials* **2003**, *24*, 4385−4415.

(22) Koshy, S. T.; Ferrante, T. C.; Lewin, S. A.; Mooney, D. J. Injectable, porous, and cell-responsive gelatin cryogels. *Biomaterials* **2014**, *35*, 2477−2487.

(23) Vandervoort, J.; Ludwig, A. Preparation and evaluation of drug-loaded gelatin nanoparticles for topical ophthalmic use. *Eur. J. Pharm. Biopharm.* **2004**, *57*, 251−261.

(24) Han, M. E.; Kang, B. J.; Kim, S. H.; Kim, H. D.; Hwang, N. S. Gelatin-based extracellular matrix cryogels for cartilage tissue engineering. *J. Ind. Eng. Chem.* **2017**, *45*, 421−429.

(25) Jeon, O.; Shin, J. Y.; Marks, R.; Hopkins, M.; Kim, T. H.; Park, H. H.; Alsberg, E. Highly elastic and tough interpenetrating polymer network-structured hybrid hydrogels for cyclic mechanical loading-enhanced tissue engineering. *Chem. Mater.* **2017**, *29*, 8425−8432.

(26) Xiao, W. Q.; He, J. K.; Nichol, J. W.; Wang, L. Y.; Hutson, C. B.; Wang, B.; Du, Y. A.; Fan, H. S.; Khademhosseini, A. Synthesis and characterization of photocrosslinkable gelatin and silk fibroin interpenetrating polymer network hydrogels. *Acta Biomater.* **2011**, *7*, 2384−2393.

(27) Fares, M. M.; Sani, E. S.; Lara, R. P.; Oliveira, R. B.; Khademhosseini, A.; Annabi, N. Interpenetrating network gelatin

methacryloyl (GelMA) and pectin-g-PCL hydrogels with tunable properties for tissue engineering. *Biomater. Sci.* **2018**, *6*, 2938−2950.

(28) Ansari, S.; Sarrion, P.; Hasani-Sadrabadi, M. M.; Aghaloo, T.; Wu, B. M.; Moshaverinia, A. Regulation of the fate of dental-derived mesenchymal stem cells using engineered alginate-GelMA hydrogels. *J. Biomed. Mater. Res., Part A* **2017**, *105*, 2957−2967.

(29) Zeng, Q. Y.; Han, Y.; Li, H. Y.; Chang, J. Bioglass/alginate composite hydrogel beads as cell carriers for bone regeneration. *J. Biomed. Mater. Res., Part B* **2014**, *102*, 42−51.

(30) Lee, K. Y.; Mooney, D. J. Alginate: Properties and biomedical applications. *Prog. Polym. Sci.* **2012**, *37*, 106−126.

(31) Huang, C. C.; Kang, M.; Shirazi, S.; Lu, Y.; Cooper, L. F.; Gajendrareddy, P.; Ravindran, S. 3D Encapsulation and tethering of functionally engineered extracellular vesicles to hydrogels. *Acta Biomater.* **2021**, *126*, 199−210.

(32) Hunt, N. C.; Hallam, D.; Karimi, A.; Mellough, C. B.; Chen, J.; Steel, D. H. W.; Lako, M. 3D culture of human pluripotent stem cells in RGD-alginate hydrogel improves retinal tissue development. *Acta Biomater.* **2017**, *49*, 329−343.

(33) Shirahama, H.; Lee, B. H.; Tan, L. P.; Cho, N. J. Precise tuning of facile one-pot gelatin methacryloyl (GelMA) synthesis. *Sci. Rep.* **2016**, *6*, No. 31036.

(34) Li, X. M.; Chen, S. W.; Li, J. C.; Wang, X. L.; Zhang, J.; Kawazoe, N.; Chen, G. P. 3D culture of chondrocytes in gelatin hydrogels with different stiffness. *Polymers* **2016**, *8*, No. 269.

(35) Hoch, E.; Hirth, T.; Tovar, G. E. M.; Borchers, K. Chemical tailoring of gelatin to adjust its chemical and physical properties for functional bioprinting. *J. Mater. Chem. B* **2013**, *1*, 5675−5685.

(36) Zhou, M. M.; Leet, B. L.; Tan, L. P. A dual crosslinking strategy to tailor rheological properties of gelatin methacryloyl. *Int. J. Bioprint.* **2017**, *3*, 130−137.

(37) Wang, S.; Maruri, D. P.; Boothby, J. M.; Lu, X.; Rivera-Tarazona, L. K.; Varner, V. D.; Ware, T. H. Anisotropic, porous hydrogels templated by lyotropic chromonic liquid crystals. *J. Mater. Chem. B* **2020**, *8*, 6988−6998.

(38) Wang, Z.; Fu, D.; Xie, D.; Fu, S.; Wu, J.; Wang, S.; Wang, F.; Ye, Y.; Tu, Y.; Peng, F. Magnetic helical hydrogel motor for directing T Cell chemotaxis. *Adv. Funct. Mater.* **2021**, No. 2101648.

(39) Sun, J. C.; Tan, H. P. Alginate-based biomaterials for regenerative medicine applications. *Materials* **2013**, *6*, 1285−1309.

(40) Dahlmann, J.; Krause, A.; Moller, L.; Kensah, G.; Mowes, M.; Diekmann, A.; Martin, U.; Kirschning, A.; Gruh, I.; Drager, G. Fully defined in situ cross-linkable alginate and hyaluronic acid hydrogels for myocardial tissue engineering. *Biomaterials* **2013**, *34*, 940−951.

(41) Boontheekul, T.; Kong, H. J.; Mooney, D. J. Controlling alginate gel degradation utilizing partial oxidation and bimodal molecular weight distribution. *Biomaterials* **2005**, *26*, 2455−2465.

(42) Young, A. T.; White, O. C.; Daniele, M. A. Rheological properties of coordinated physical gelation and chemical crosslinking in gelatin methacryloyl (GelMA) hydrogels. *Macromol. Biosci.* **2020**, *20*, No. e2000183.

(43) LaNasa, S. M.; Hoffecker, I. T.; Bryant, S. J. Presence of pores and hydrogel composition influence tensile properties of scaffolds fabricated from well-defined sphere templates. *J. Biomed. Mater. Res., Part B* **2011**, *96b*, 294−302.

(44) Chiu, Y. C.; Kocagoz, S.; Larson, J. C.; Brey, E. M. Evaluation of physical and mechanical properties of porous poly (Ethylene GLYCOL)-co-(L-lactic acid) hydrogels during degradation. *PLoS One* **2013**, *8*, No. e60728.

(45) Dou, Q. Q.; Low, Z. W. K.; Zhang, K. Y.; Loh, X. J. A new light triggered approach to develop a micro porous tough hydrogel. *RSC Adv.* **2017**, *7*, 27449−27453.

(46) Chen, Y. C.; Lin, R. Z.; Qi, H.; Yang, Y.; Bae, H.; Melero-Martin, J. M.; Khademhosseini, A. Functional human vascular network generated in photocrosslinkable gelatin methacrylate hydrogels. *Adv. Funct. Mater.* **2012**, *22*, 2027−2039.

(47) Kadri, R.; Ben Messaoud, G.; Tamayol, A.; Aliakbarian, B.; Zhang, H. Y.; Hasan, M.; Sanchez-Gonzalez, L.; Arab-Tehrany, E. Preparation and characterization of nanofunctionalized alginate/

methacrylated gelatin hybrid hydrogels. *RSC Adv.* **2016**, *6*, 27879−27884.

(48) Koehler, J.; Brandl, F. P.; Goepferich, A. M. Hydrogel wound dressings for bioactive treatment of acute and chronic wounds. *Eur. Polym. J.* **2018**, *100*, 1−11.

(49) Deng, J.; Cheng, C.; Teng, Y. Y.; Nie, C. X.; Zhao, C. S. Mussel-inspired post-heparinization of a stretchable hollow hydrogel tube and its potential application as an artificial blood vessel. *Polym. Chem.* **2017**, *8*, 2266−2275.

(50) Bai, X.; Gao, M. Z.; Syed, S.; Zhuang, J.; Xu, X. Y.; Zhang, X. Q. Bioactive hydrogels for bone regeneration. *Bioact. Mater.* **2018**, *3*, 401−417.

(51) Leor, J.; Amsalem, Y.; Cohen, S. Cells, scaffolds, and molecules for myocardial tissue engineering. *Pharmacol. Ther.* **2005**, *105*, 151−163.

(52) Khademhosseini, A.; Vacanti, J. P.; Langer, R. Progress in tissue engineering. *Sci. Am.* **2009**, *300*, 64−71.

(53) Park, H.; Guo, X.; Temenoff, J. S.; Tabata, Y.; Caplan, A. I.; Kasper, F. K.; Mikos, A. G. Effect of swelling ratio of injectable hydrogel composites on chondrogenic differentiation of encapsulated rabbit marrow mesenchymal stem cells in vitro. *Biomacromolecules* **2009**, *10*, 541−546.

(54) Bitar, M.; Brown, R. A.; Salih, V.; Kidane, A. G.; Knowles, J. C.; Nazhat, S. N. Effect of cell density on osteoblastic differentiation and matrix degradation of biomimetic dense collagen scaffolds. *Biomacromolecules* **2008**, *9*, 129−135.

(55) Kessler, L.; Gehrke, S.; Winnefeld, M.; Huber, B.; Hoch, E.; Walter, T.; Wyrwa, R.; Schnabelrauch, M.; Schmidt, M.; Kuckelhaus, M.; Lehnhardt, M.; Hirsch, T.; Jacobsen, F. Methacrylated gelatin/hyaluronan-based hydrogels for soft tissue engineering. *J. Tissue Eng.* **2017**, *8*, 1−14.

(56) Liu, J.; Tagami, T.; Ozeki, T. Fabrication of 3D-printed fish-gelatin-based polymer hydrogel patches for local delivery of PEGylated liposomal doxorubicin. *Mar. Drugs* **2020**, *18*, No. 325.